

The high-pressure monazite-to-scheelite transformation in CaSeO_4

W. A. CRICHTON^{1,2,*}, M. MERLINI³, H. MÜLLER¹, J. CHANTEL¹ AND M. HANFLAND¹

¹ European Synchrotron Radiation Facility, 6 rue Jules Horowitz, 38043 Grenoble Cedex, France

² Department of Earth Sciences, University College London, Gower Street, London WC1E 6BT, UK

³ Dipartimento di Scienze della Terra “Ardito Desio”, Università degli Studi di Milano, via Mangiagalli 34, 20133 Milano, Italy

[Received 2 December 2011; Accepted 1 March 2012; Associate Editor: G. Diego Gatta]

ABSTRACT

The high-pressure monazite–scheelite structure transition has been observed at $P > 4.57$ GPa in CaSeO_4 by synchrotron X-ray powder diffraction. It is a first-order transition with a 4.5% volume change and is severely hindered kinetically. Scheelite-type CaSeO_4 remains to a maximum experimental pressure of 42.2 GPa and no (002) reflection, specifically indicative of a subgroup transition to a fergusonite-type structure, is observed. Scheelite-type CaSeO_4 remains at ambient conditions, where the tetragonal unit cell has parameters of $a = 5.04801(11)$ $c = 11.6644(5)$ Å and $V = 297.21(3)$ Å³ with $D_{\text{calc}} = 4.090$ g cm^{−3}. The diffraction pattern of the recovered material was refined in space group $I4_1/a$ to $R_p = 0.98\%$, $wR_p = 1.91\%$, $\text{GoF} = 0.59$, $R_{\text{Fobs}} = 5.04\%$, $wR_{\text{Fobs}} = 4.27\%$. The oxygen is located on the general 16f site at (0.2578(8) 0.3699(14) 0.5755(4)) and shares four identical bonds with Se ($4a$: $\frac{1}{2}$ $\frac{1}{2}$ $\frac{1}{2}$) at 1.644(5) Å. The Ca ($4b$: 0, 0, $\frac{1}{2}$) is eight-coordinated via O at $4 \times 2.440(6)$ Å and $4 \times 2.504(5)$ Å. This is further evidence of the dissimilarity of sulfate and selenate at high pressure and temperature conditions and the closer resemblance of the selenates to the orthophosphates, arsenates and vanadates, where this type of transition sequence has been described.

KEYWORDS: scheelite, monazite, high pressure, powder diffraction, synchrotron.

Introduction

In the last decade considerable efforts have been made to discover new structural associations, properties and non-ambient behaviours of monazite- and scheelite-type compounds due to their technological utility. Scheelite, CaWO_4 (e.g. Grzechnik *et al.*, 2003), is a tetragonal 8–4 coordinated mineral found in hydrothermal veins and skarns, where it is commonly associated with wolframite and other large cation refractory minerals. The scheelite structure is shared by relatively few minerals; examples include stolzite,

PbWO_4 , wulfenite, PbMoO_4 , powellite, CaMoO_4 and reidite, a high pressure ZrSiO_4 (zircon) polymorph that is found in impact breccias (Reid and Ringwood, 1969; Liu, 1979; Marques *et al.*, 2009). Raspite is a polymorph of stolzite, but it is structurally unique with no other composition sharing its topology in any conditions (Fujita *et al.*, 1977). The scheelite structure is widely reported in synthetic compounds due to its ability to form compounds with valence variations from $A^{1+}B^{7+}\text{O}_4$ to $A^{4+}B^{4+}\text{O}_4$. Oxides crystallizing with $B = \text{W}, \text{Mo}, \text{V}, \text{Nb}, \text{Cr}, \text{Re}, \text{I}, \text{Ge}$ and Si have been described (e.g. Liu and Bassett, 1986) and other stoichiometries are known for chloride, fluoride and hydride systems.

In mineralogy the term monazite is used to describe a group of monoclinic lanthanide orthophosphates, Levinson modifiers are used

* E-mail: crichton@esrf.fr

DOI: 10.1180/minmag.2012.076.4.08

identify the individual members of the group, so that in monazite-(La), for example, lanthanum is the dominant element at the appropriate structural site. A wide variety of minerals with the monazite structure have been described; they include arsenates and chromates with large cations such as gasparite, (Ce,REE)AsO₄, rooseveltite, BiAsO₄, and crocoite, PbCrO₄. Monazite from placers and other deposits, has the potential to be a significant primary ore of rare-earth elements and thorium, though this strategic industrial process is not yet well developed on a worldwide scale. Monazites can be transformed to other structure types, or decomposed into their constituent components under appropriate conditions. A thorough treatise covering the crystal chemistry of most monazites, and transitions to and from them, can be found in Clavier *et al.* (2011).

It has been shown experimentally that CaSO₄ undergoes a transition from its anhydrite form to the monazite structure at high pressure (Stephens, 1964; Borg and Smith, 1975). Crichton *et al.* (2005) reported that monazite-type CaSeO₄ remained stable at pressures up to 11.8 GPa (though they made no claim to observe the transition at this pressure, deferring to the work of Borg and Smith (1975) for a transition pressure of above 2 GPa; see also Gracia *et al.*, 2012; Ma *et al.*, 2007). It has also been shown that CaSO₄ transforms to a baryte-type structure at high pressure and temperature (Crichton *et al.*, 2005) and this has been investigated by density functional theory (DFT) calculations (Gracia *et al.*, 2012) and largely reproduces the experimental observations, without locating the distorted baryte, AgMnO₄-type, intermediate. The monoclinic distortion in this structure is subtle but may nonetheless be expected from similar behaviour in perchlorate and permanganate systems, as identified by Pistorius *et al.* (1969). This example of CaSO₄ achieving a baryte-type structure serves as another success of the oft-used rule of thumb of going down a group in the periodic table (Ca to Ba), or increasing ‘chemical pressure’, as a proxy for extrinsic compression. Barium sulfate has been studied several times recently. It has been shown that baryte undergoes at least one phase transition to a structure, or structures, previously reported as tentatively triclinic (Lee *et al.*, 2001) and orthorhombic $P2_12_12_1$ (Santamaria-Pérez *et al.*, 2011) at a range of pressures (13 GPa to 27 GPa; 32 GPa by calculation, Santamaria-Pérez *et al.*, 2011) which appear related to the state of hydrostaticity of the measurements. From the

experimental work carried out under the most favourable hydrostatic environments, i.e. in helium, the transition must be located at pressures above 21.8 GPa, as it was not observed at the maximum pressure reached by the single-crystal study reported by Crichton *et al.* (2011). Subsequent powder data collections in helium suggest a transition pressure of 27 GPa (Santamaria-Pérez *et al.*, 2011). It is unclear whether the reported triclinic phase and the post-baryte $P2_12_12_1$ structure are the same. The demonstration that CaSeO₄ also forms a monazite, via rhabdophane-like intermediates, upon complete loss of water from its gypsum-type dihydrate is available in these pages (Crichton *et al.*, 2010) and lends further credence to the structural similarity between sulfates and selenates. Indeed, CaSeO₄ is in some regard an intermediate to the anhydrite form of the sulfate and the baryte structure occurring at high pressure in CaSO₄, or, at ambient pressure, in BaSO₄. However, despite the fact that this same selenate form has been previously described (with caveats) as an orthorhombic $P2_12_12_1$ structure, it should not be confused with, and a CaSeO₄-type designation should not be applied to, an orthorhombic post-baryte form of BaSO₄, CeVO₄ or CaSO₄ with the same $P2_12_12_1$ symmetry; they are not the same (see also Santamaria-Pérez *et al.*, 2011; Errandonea *et al.*, 2011; Gracia *et al.*, 2012).

High-pressure and/or high-temperature relations in various chemistries dictate that scheelites are most commonly formed from zircon- and monazite-type structures and that these may themselves transform to the fergusonite, YNbO₄-type structure (Grzechnik *et al.*, 2003, 2005) or decompose to their constituents, possibly related to underlying phase transitions in these component phases (Liu, 1979; Grzechnik *et al.*, 2004; Crichton *et al.*, 2009). A discrete post-fergusonite phase is not described. Scheelite-type structure have not been described for sulfates or selenates despite the facts that monazite forms are known for both, and that scheelite is a common post-monazite transition product (Snyman and Pistorius, 1963; Stephens, 1964; Borg and Smith, 1975; Crichton *et al.*, 2005; Bradbury and Williams, 2009; Crichton *et al.*, 2010; Clavier *et al.*, 2011). A summary of structure-types for related chemistries can be found in Table 1. Tellurates form diverse structures of e.g. CaUO₄-type (Hottentot and Loopstra, 1979), which do not form part of this extended general

TABLE 1. The positively identified structure-types of sulfates, selenates and related chemistries at ambient and high pressure in the literature.

<i>M</i> Composition	Sulfate	Chromate	Selenate	Molybdate	Tungstate
Cd	CdSO ₄ , CdVO ₄	CdVO ₄ , CoMoO ₄	n.d.	CaWO₄	NiWO ₄
Ca	CaSO₄ , CePO₄ , AgMnO₄ , BaSO₄ , P2₁2₁2₁	ZrSiO ₄ , CePO₄ , CaWO₄	CePO₄ , CaWO₄	CaWO₄ , YNbO ₄	CaWO₄ , YNbO ₄
Hg	CdSO ₄	CrVO ₄ , AgMnO ₄	CdSO ₄	HgMoO ₄	HgMoO ₄
Sr	BaSO₄ , BaSO ₄ (HT)	CePO₄ , NdTaO ₄	CePO₄	CaWO₄ , YNbO ₄	CaWO₄ , YNbO ₄
Pb	BaSO₄	CePO₄ , BaSO₄	CePO₄	CaWO₄	CaWO₄ , YNbO ₄ , PbWO ₄
Ba	BaSO ₄ , BaSO ₄ (HT), P2₁2₁2₁	BaSO₄	BaSO₄	CaWO₄ , YNbO ₄	PbWO ₄ (mP48)
Lanthanide, Y	BaSO ₄	CePO₄ [†] , ZrSiO ₄ [†] , CaWO₄ [‡]	n.d.	CaWO₄ [†]	CaWO₄ , YNbO ₄ , PbWO ₄ (mP48)
					n.d.
	Silicate/Germanate	Phosphate	Vanadate		
Lanthanide, Y	ZrSiO ₄ [‡]	ZrSiO ₄ [†] , CePO₄ [†] , CaWO₄ ^{†‡}	ZrSiO ₄ ^{†‡} , CePO₄ ^{†‡} , CaWO₄ [†] , YNbO ₄ [†] , P2₁2₁2₁		
Th	ZrSiO ₄ [‡] , CePO₄ [‡] , CaWO₄ [‡]				

To our knowledge CaSO₄ as AgMnO₄- and CeVO₄ as CaWO₄-type have yet to be refined, and PbWO₄(mP48) and CaSO₄ as BaSO₄-type required high temperatures for transformation.

Associations in bold are shared between chemistries that exhibit the same structure-types as CaSO₄ and CaSeO₄.

Where no distinct phase is identified, it is noted as n.d.

[†] For trivalent *M*³⁺ sites and pentavalent tetrahedral sites.

[‡] For tetravalent *M*⁴⁺ sites and tetravalent tetrahedral sites.

scheme, as they are higher coordinated 6–8 structures and therefore lack the tetrahedral sulfate and selenate groups that define these and related topologies.

What then for CaSeO_4 at high load: chemical pressure via substitution of Se for S and reducing the pressure to reach a high-pressure baryte-type structure? For CaSO_4 , BaSO_4 and BaSeO_4 all form baryte and BaSeO_4 is also known as a monazite. Or, structural similitude with the other monazites and obtain a scheelite, for the monazite-scheelite transition is also described, see Clavier *et al.* (2011) for examples. It is unclear from systematic behaviour, now most commonly expressed in terms of the variations upon the diagrams first produced by Muller *et al.* (1969) (who would have CaSeO_4 as a borderline monazite-zircon), Bastide (1987) (who has similar, and scheelite at high P), or Fukunaga and Yamaoka (1979) (who would have baryte as a post-monazite), exactly what should happen. One clue is given by the only other mention of CaSeO_4 as a scheelite in the literature, as the star-graded JCPDS card number 36-0293. This card states that the compound was formed through evaporation of a solution of CaCO_3 in selenic acid. This method produced a monazite in our case: it is equivalent to ‘Procedure B’ of Crichton *et al.* (2010) and may indicate that the monazite–scheelite transition occurs at high temperature (through forced evaporation), and as scheelite is invariably denser than monazite, this would imply a negative Clapeyron slope. Therefore, we should cross this same transition as the pressure is increased.

To this end we have undertaken measurements to determine the post-monazite form crystallizing at high pressure in CaSeO_4 . We describe the observed transition and detail structural features of the recovered sample at ambient conditions for direct comparison of both monazite and scheelite forms under the same conditions.

Experimental

The starting material was prepared from a batch of synthetic gypsum-type $\text{CaSeO}_4 \cdot 2\text{H}_2\text{O}$ by heating overnight in air at 600°C. This produced a fine powder, which was checked to be pure monazite-type CaSeO_4 on a Miniflex-II lab diffractometer. The sample was subsequently loaded, along with a ruby for pressure measurement (Forman *et al.*, 1972), in a membrane-driven diamond-anvil cell equipped with 300/250 μm culet diamonds and a steel gasket with an initial

hole diameter of 150 μm and thickness of 36 μm . The pressure-transmitting medium was helium. High pressure measurements were made at beamline ID09A at the ESRF, using a focussed X-ray beam from a bent Laue monochromator operating at 30 keV. Two-dimensional diffraction patterns were collected on a mar555 flat-panel detector at a distance of 310 mm from the sample and were corrected and integrated to conventional one-dimensional 2θ -intensity datasets using *fit2d* software (Hammersley *et al.*, 1996), after integration parameters were established using a silicon powder standard, Hammersley *et al.* (1994). Diffraction datasets were fitted using *Jana2006*, Petricek *et al.* (2006).

Measurements at high pressure

The results of refinements of the monazite-type phase up to 4.2 GPa are shown in Fig. 1. The unit cell compresses smoothly, with the b axis (green) and c axis (blue) showing identical compressibility and the a axis (red) being fractionally more compressible. These can be quantified as axial moduli after fitting an equation-of-state (EoS) formalism to the cube of the cell-length measurements and this results in $K_a = 57.1(2)$ GPa, $K_b = 65.2(12)$ GPa and $K_c = 67.8(10)$ GPa. The β angle reduces linearly at a rate of $-7.60(3)10^{-4}^\circ \text{ GPa}^{-1}$. A similar fit of a second-order Birch–Murnaghan EoS to the volumetric data results in $V_0/Z = 78.328(5) \text{ \AA}^3$ and $K_T = 69.1(7)$ GPa. This value is approximately 60% of the bulk modulus of monazite, CePO_4 , at 109 GPa (Huang *et al.*, 2010), which is one third more dense with $D = 5.23 \text{ g cm}^{-3}$. Comparing this with models of predicted bulk moduli (e.g. Hazen and Finger, 1982), using the average Ca–O bond length at ambient of 2.513 \AA , a bulk modulus of ~ 77 GPa is obtained, which is no better than a fair approximation.

Upon further increase in pressure, Fig. 2, we observe the growth of a small peak (at 5.2° , asterisked in Fig. 2). It was not, however, until several GPa (and hours) later that the peaks became sufficiently distinct from the monazite to produce definite data on the nature of this transition and even at the highest pressure, monazite-type peaks were still observed (though they could not be identified without prior information). This sluggish transition is typical of these oxide materials, though admittedly this is the most extreme case we have encountered in our exploration of these materials to date. We point

HIGH PRESSURE MONAZITE-TO-SCHEELITE TRANSFORMATION

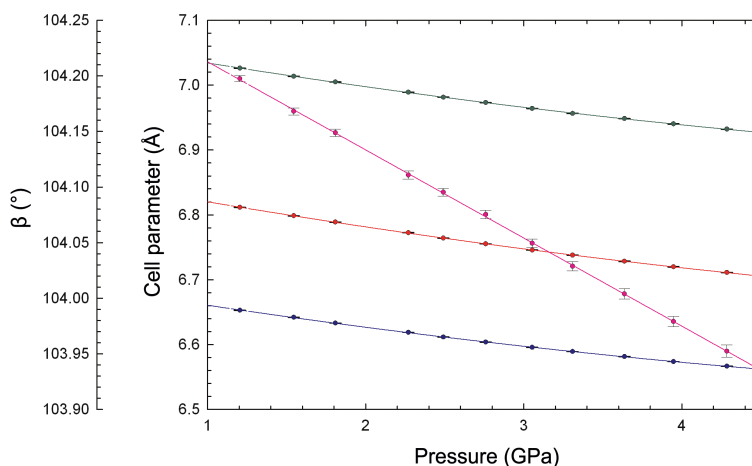


FIG. 1. The results of powder diffraction refinements of the monazite-type phase at pressures up to 4.2 GPa, showing the smooth variation of the a -, b - and c -cell parameters as a function of pressure in red, green and blue respectively and the linear decrease of the β angle in pink.

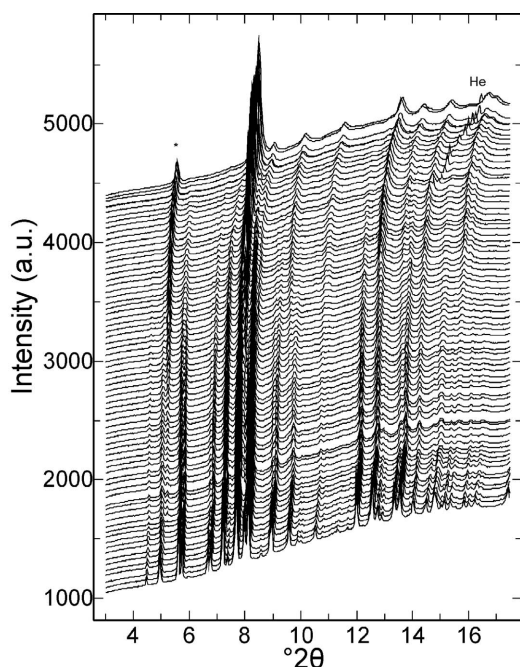


FIG. 2. Stacked diffraction patterns showing the change from the monazite (bottom) to scheelite (top) structures. The onset of the transition can be seen by the appearance of the small peak at $\sim 5.2^\circ$, which is asterisked. The small peaks visible at higher angles are due to He, the pressure-transmitting medium, and are marked 'He'.

out that this situation would probably be improved by heating; however, this is unavailable to a He-loaded cell. As we increased the pressure further, up to 42 GPa, we were particular to the observation of a weak low-angle peak that would correspond to the extinct (002) of scheelite, which is indicative of the transition to the subgroup ($I2/a$) fergusonite phase (e.g. Grzechnik *et al.*, 2003). This test proved negative and we decompressed to ambient and recovered the sample for further comparisons with monazite at room conditions.

A Le Bail fit (Le Bail *et al.*, 1988) of the recovered-to-ambient sample converged to $R_p = 4.73\%$, $wR_p = 8.47\%$, with a GoF = 0.94 using 4243 reflections, 12 parameters (5 profile, 5 background, a and c) and one constraint ($b = a$) in $P1$ with metric tetragonal cell parameters. It was evident from this fit that some monazite phase was also present. Nevertheless, as a test of data robustness, the symmetry was assessed (I -centred lattices and the $I4_1/a$ space group offered little degradation of the quality of fit parameters, and had the highest ratio of reflections extinct/generated of about $\frac{1}{2}$) and the structure was solved using the charge-flipping method, with the input of the chemistry and $Z = 4$ into an otherwise default *Superflip* run (Palatinus and Chapuis, 2007). The *Expo* suite of programs (Altomare *et al.*, 1999) was also used to solve the structure directly from the same set of extracted intensities, with a final refined $R = 6.07\%$ (groups/parameters = 5.50). This was used as an initial model for a

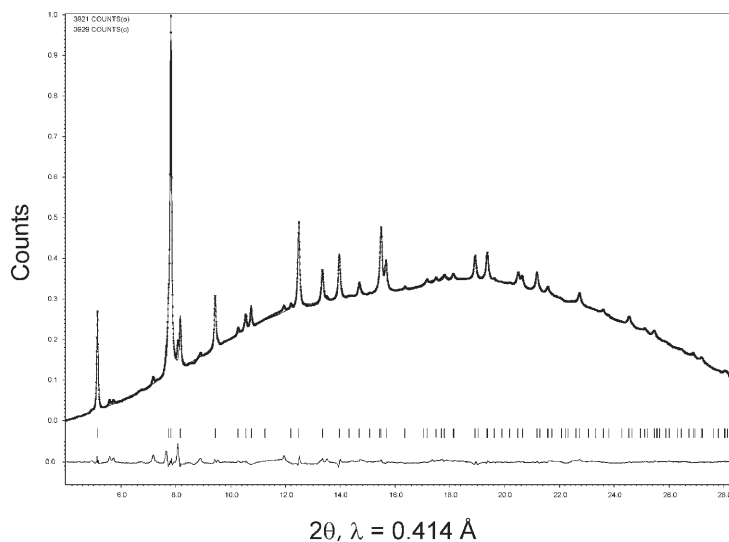


FIG. 3. A *Jana2006* refinement of scheelite-type CaSeO_4 upon recovery to ambient conditions. The background has been set as $y_{\min} = 0$. Peaks from a small contribution of monazite are visible in the misfit and are ignored in final refinement.

Rietveld refinement, which converged rapidly (Fig. 3) and produced the parameters listed in Tables 2 to 5 and the structure shown in Fig. 4.

Discussion

This is the fourth Ca-containing oxide scheelite reported after the tungstate, scheelite *proper*

(CaWO_4), the molybdate powellite (CaMoO_4), and a high pressure form of the chromate, chromatite (CaCrO_4 ; Long *et al.*, 2006). Compared to the data available for these chemistries, scheelite-type CaSeO_4 has a significantly shorter tetrahedral bond length, indeed the shortest described for a scheelite, of $4 \times 1.644(4) \text{ \AA}$, due to the ionic radius of IVSe^{6+}

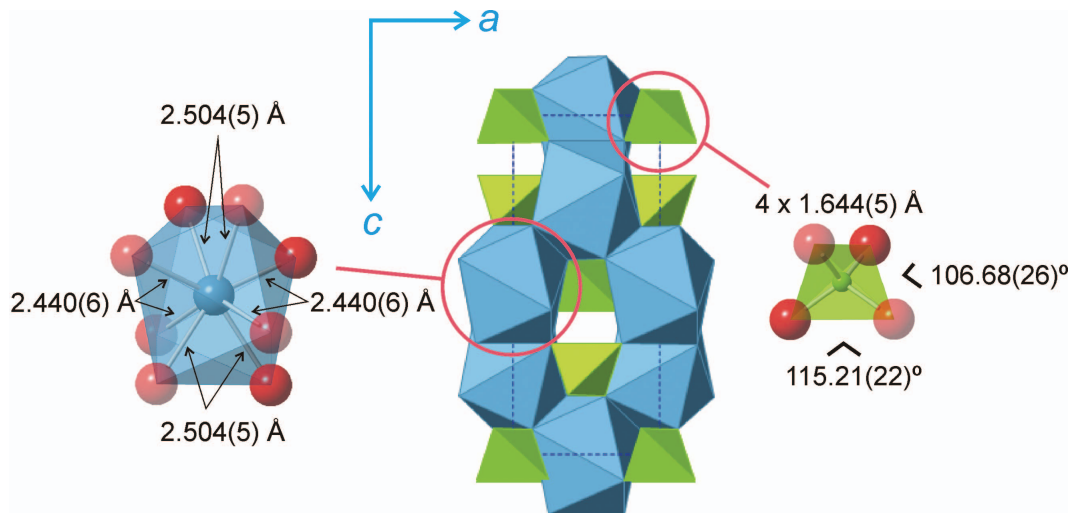


FIG. 4. The refined-at-ambient structure of scheelite-type CaSeO_4 with the 8- and 4-fold coordination polyhedra of Ca and Se shown in blue and green, respectively. The bond lengths and angles are indicated.

TABLE 2. Crystallographic parameters for recovered scheelite-type CaSeO_4 .

Space group	$I4_1/a$
Unit cell dimensions	$a = 5.04801(11) \text{ \AA}$ $c = 11.6644(5) \text{ \AA}$
V	$297.24(2) \text{ \AA}^3$
Z	4
Density	4.090 g cm^{-3}
Absorption coefficient	3.350 mm^{-1}

The refinement parameters are as follows: $R_{\text{obs}} = 5.04\%$, $wR_{\text{obs}} = 4.27\%$, $R_{\text{all}} = 5.46\%$, $wR_{\text{all}} = 4.38\%$. The profile contained 4306 reflections, with a GoF = 0.59, an $R_p = 0.98\%$ and $wR_p = 1.91\%$. The number of parameters refined were the above (eight) plus 15 background, five profile and overall scale. The minor monazite content was ignored, but not excluded and the Compton background from diamonds was not subtracted; y_{min} was set to 0.

being about half of that of $^{\text{IV}}\text{W}^{6+}$ and $^{\text{IV}}\text{Mo}^{6+}$ ($\text{W}-\text{O}$ and $\text{Mo}-\text{O}$ at $\sim 1.78 \text{ \AA}$), and, we note, it is identical to that of the average $\text{Se}-\text{O}$ length for the monazite form at standard conditions, at 1.644 \AA (Crichton *et al.*, 2010). In fact, we identify that not only is the average bond length of the scheelite selenate the same as in its monazite form; the volume of the scheelite-type SeO_4 unit is 2.262 \AA^3 (compared to 2.260 \AA^3 for the monazite-type structure). The average tetrahedral bond angle is 109.50° (compared to 109.43°), with a variance of 19.37 (22.78) and a mean quadratic elongation is 1.005 (1.006). The $\text{Ca}-\text{O}$ bond lengths, which are of a similar order ($4 \times 2.440(4) \text{ \AA} + 4 \times 2.504(5) \text{ \AA}$; average 2.470 \AA) are not dissimilar to the other Ca-containing scheelites and define an 8-coordinated polyhedron with a volume of 26.83 \AA^3 (compared to 27.03 \AA^3 , for the CaSeO_4 monazite, or

26.72 \AA^3 for CaWO_4). Scheelite-type CaSeO_4 has, on average, shorter bonds with less distortion than monazite-type CaSeO_4 , where the range is $2.395\text{--}2.686 \text{ \AA}$. There are no refinements of scheelite-type CaCrO_4 but, given that the ionic radius of $^{\text{IV}}\text{Cr}^{6+}$ is comparable (0.26) to that of Se (0.28), we would assume bond lengths of $\leq 1.644 \text{ \AA}$ for $\text{Cr}-\text{O}$, similar $\text{Ca}-\text{O}$ lengths and slightly smaller cell parameters and compressibility for the scheelite-structured chromate. The tetrahedral $\text{Cr}-\text{O}$ bond length of 1.647 \AA in zircon-structured CaCrO_4 further supports this notion. Using these similarities, it can be estimated that CaCrO_4 would have a density of 3.48 g cm^{-3} at ambient conditions, which is 16% denser than the zircon form and 5% more than a hypothetical monazite form, should it exist. Long *et al.* (2006) have estimated the ambient volume of scheelite-type CaCrO_4 at ambient conditions as $299.5 \pm 2.0 \text{ \AA}^3$. This is very close to our value for CaSeO_4 , at $297.24(2) \text{ \AA}^3$, Table 1. We would then propose that there should be significant opportunity for solid solution in mixed $\text{Ca}(\text{Cr},\text{Se})\text{O}_4$ chemistries and that, furthermore, Se might be used to stabilize a Cr-rich monazite and, conversely, Cr may stabilize a Se-containing zircon. Such compositions remain to be described.

Given the list of similarities between these structures and chemistries, it becomes clear that it is in polyhedral contacts, in the packing of these subunits, where any contrast between the monazites and the scheelites must be significant. In the scheelite structure, each Ca-polyhedron edge-shares to its four adjacent and symmetrically identical units and each Se-tetrahedron is fully corner-shared to these. In the monazite structure there is only edge-sharing from one CaO_8 polyhedron to its adjacent CaO_8 unit and a SeO_4 tetrahedron; the remaining liaisons are corner-shared via a bridging apical oxygen. The space occupied by the polyhedral units in the unit cell

TABLE 3. Atom coordinates and equivalent displacement parameters (\AA^2) for scheelite-type CaSeO_4 .

Atom	Site	x/a	y/b	z/c	U_{eq}
Se	4a	$\frac{1}{2}$	$\frac{1}{2}$	$\frac{1}{2}$	0.0101(9)
Ca	4b	0	0	$\frac{1}{2}$	0.022(2)
O	16f	0.2578(8)	0.3699(14)	0.5755(4)	0.027

The space group $I4_1/a$ has a further setting and, when transformed this gives Ca located at 0, $\frac{1}{4}$, $\frac{1}{8}$; Se at $\frac{1}{2}$, $\frac{3}{4}$, $\frac{1}{8}$ and O at 0.2574, 0.6212, 0.0482.

TABLE 4. Displacement parameters (\AA^2) for scheelite-type CaSeO_4 .

Atom	U_{11}	U_{22}	U_{33}	U_{23}	U_{13}	U_{12}
Se	0.0103(14)	0.0103(14)	0.0099(19)	0	0	0
Ca	0.013(3)	0.013(3)	0.040(5)	0	0	0
O	0.022(6)	0.040(8)	0.019(7)	−0.002(6)	0.001(4)	−0.013(4)

amounts to 49% in the scheelite structure (146.2 \AA^3 of 297.2 \AA^3) and 47% (146.2 of 310.2 \AA^3) in the monazite at ambient conditions. This represents a reduction of void space of $\sim 4\%$. Indeed, the volume change upon transition was estimated from the degree of volumetric compression (Fig. 5) at the onset pressure of 4.57 GPa to be $\sim 4.5\%$.

Refinement of the structures was not prudent in the strongly mixed region, except from a few points obtained on decompression (those at less than 20 GPa). Nonetheless, the extracted unit-cell values of the scheelite cell exhibit smooth compression. Fitting of a third-order EoS to the axial and volumetric data highlights a 45% difference in the compressibility of the a and c axes, at $K_a = 97.6(12)$ GPa, $K'_a = 5.38(13)$ and $K_c = 67.2(17)$ GPa, $K'_c = 4.22(17)$. Comparison of volumetric data of this scheelite, where fitted $V_0/Z = 74.3103(13) \text{ \AA}^3$, $K_T = 84.2(5)$ GPa and $K' = 5.00(5)$, with others shows that it is most similar to CaMoO_4 powellite, at 82.5(7) GPa (Crichton and Grzechnik, 2004), which also has the more comparable average Ca–O distance of any scheelite at 2.458 \AA , cf. $\sim 2.472 \text{ \AA}$ here. Both these values are higher than that obtained for the tungstate scheelite, where $K_T = 74(6)$ GPa and $K' = 3.89(10)$, Grzechnik *et al.* (2003), though again the average bond length is similar, Ca–O8 = 2.459 \AA . These values are somewhat surprisingly at odds with those for scheelite-type CaCrO_4 , where K_T has been estimated at 125.1 ± 6.2 GPa by Long *et al.* (2006).

Therefore, CaSeO_4 displays a transition sequence that can be described as closely

resembling those of the orthophosphates. We have previously shown that CaSeO_4 has rhabdophane-like intermediates on partial dehydration, on full dehydration it is a monazite and at high pressure it forms a scheelite. Calcium sulfate also shows both rhabdophane-like structures (γ - CaSO_4 , bassanite) and monazite forms; i.e. structures with topologies that are common to natural orthophosphates; but, in contrast, at high load it reverts to the baryte-type structure. Consequently, the monazite–scheelite rule-of-thumb breaks down but the anhydrite–baryte does not, indicating that sulfates (selenates) are particularly sensitive to our description in systematic trends. Other than those structures mentioned above this same monazite–scheelite transition sequence might be expected for both the large divalent cation selenates SrSeO_4 and PbSeO_4 , which are monazites (Effenberger and Pertlik, 1986), especially when Sr and Pb tungstates and molybdates are already described as scheelites. However, despite the similarities of the selenates with CaCrO_4 , SrCrO_4 and PbCrO_4 (Effenberger and Pertlik, 1986; Pistorius and Pistorius, 1962), only full structural descriptions exist for scheelite-type chromates with M^{3+} lanthanide chemistries (i.e. post monazites, with nominal pentavalent, rather than hexavalent Cr, as above). A similar situation occurs for the smaller transition metal selenates that crystallize in the CrVO_4 -type structure, also known as NiSO_4 -type, when $M = \text{Mg, Ni, Cu, Cr}$; as, only nominal V^{5+} scheelites are described, and it therefore seems unlikely that these will produce scheelite-type structures at high load. Other transition-metal selenates crystallize in the CuSO_4 -type (also known as ZnSO_4 -type) and these are proto- CrVO_4 structures. The almost ubiquitous prevalence for pentavalent chemistries in scheelite-type Cr- and V-containing systems might therefore be a limiting condition for further exploration in that direction, in spite of the similarity between the structures of CaCrO_4 and CaSeO_4 .

Regarding other selenates, we might expect CoMoO_4 -type structures for those smaller

TABLE 5. Selected interatomic distances and angles for scheelite-type CaSeO_4 .

Se–O	1.644(5)	O–Se–O'	106.68(26)
Ca–O	2.440(6)	O'–Se–O''	115.21(22)
Ca–O	2.504(5)		

HIGH PRESSURE MONAZITE-TO-SCHEELITE TRANSFORMATION

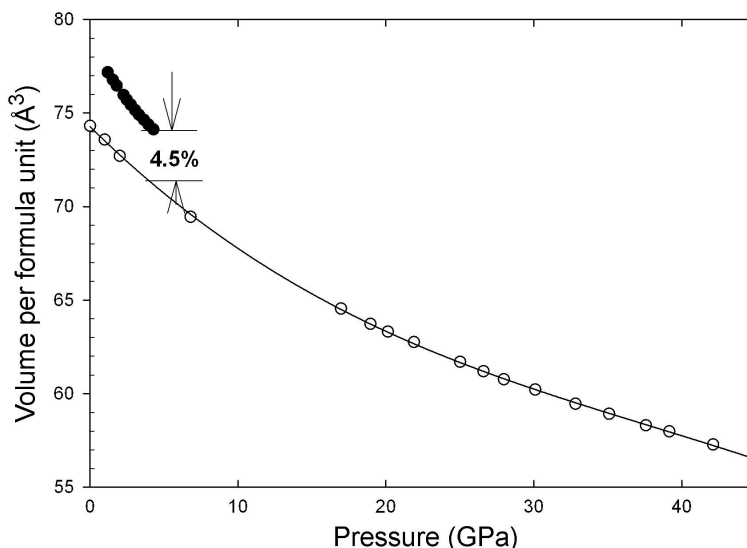


FIG. 5. Volumetric compression, shown as V/Z vs. P , showing the 4.5% volume difference between monazite and scheelite at the transition onset (4.57 GPa).

$M^{2+}\text{SeO}_4$ transition metal selenates that are described (as per MgCrO_4 , MgMoO_4 and CdCrO_4 , NiSO_4 , NiCrO_4 , NiMoO_4). Given that a post- CoMoO_4 -type structure would probably involve the NiWO_4 -type (e.g. wolframite, MgWO_4 , NiMoO_4), something rather special must happen to smaller cation M^{2+} selenates, as we are unaware of any simple hexavalent and octahedral Se-containing oxide at all. Following known tungstate and silicate behaviour, such extreme coordinations may necessitate decomposition. Alternatives may be available for larger cations, through following the lead of using lanthanides, we might envisage stabilizing tetravalent Se compounds such as $M^{3+}\text{HSe}^{4+}\text{O}_4$. Further options for encountering zircon-, monazite- or scheelite-like topologies may also make use of the structural similarity of the lone-pair-active $M^{2+}\text{Se}^{4+}\text{O}_3$ compounds with their $M^{2+}\text{Se}^{6+}\text{O}_4$ equivalent, such as in CaSeO_3 or SrSeO_3 e.g. Wildner and Giester (2007), Lipp and Schleid (2008).

Conclusion

We have compressed calcium selenate from its monazite structure up to and through the kinetically limited transition to the scheelite form. The recovered high pressure phase is identified as of scheelite type and the density

difference is some 4.5% at the onset of the transition and 5% greater than that of monazite at 3.880 g cm^{-3} in standard conditions. The cell parameters obtained here are identical to those of JCPDS 36-0293 to 1:10k, confirming that scheelite-type CaSeO_4 can be formed by both wet chemical and high-pressure routes.

Acknowledgements

The X-ray diffraction data were collected during beamtime allocated to in-house research at ID09A; WAC would also like to take this opportunity to acknowledge the outstanding contribution the former Principal Editor of *Mineralogical Magazine*, Dr Mark Welch, made to the journal. The authors appreciate the comments of two anonymous reviewers, whose input improved the clarity of previous versions of the manuscript.

References

- Altomare, A., Burla, M.C., Camalli, M., Carrozzini, B., Cascarano, G.L., Giacovazzo, C., Guagliardi, A., Moliterni, A.G.G., Polidori, G. and Rizzi, R. (1999) *EXPO*: a program for full pattern decomposition and structure solution. *Journal of Applied Crystallography*, **32**, 339–340.
- Bastide, J.P. (1987) Simplified systematics of the

- compounds ABX₄ (X= O²⁻, F⁻) and possible evolution of their crystal structures under pressure. *Journal of Solid State Chemistry*, **71**, 115–120.
- Borg, I.Y. and Smith, D.K. (1975) High-pressure polymorph of CaSO₄. *Contributions to Mineralogy and Petrology*, **50**, 127–133.
- Bradbury, S.E. and Williams, Q. (2009) X-ray diffraction and infrared spectroscopy of monazite-structured CaSO₄ at high-pressures: implications for shocked anhydrite. *Journal of Physics and Chemistry of Solids*, **70**, 134–141.
- Clavier, N., Podor, R. and Dacheux, N. (2011) Crystal chemistry of the monazite structure. *Journal of the European Ceramic Society*, **31**, 941–976.
- Crichton, W.A., and Grzechnik, A. (2004) Crystal structure of calcium molybdate, CaMoO₄, a scheelite-type to fergusonite-type transition in powellite at *P* > 15 GPa. *Zeitschrift für Kristallographie – New Crystal Structures*, **219**, 337–338.
- Crichton, W.A., Parise, J.B., Antao, S.M. and Grzechnik, A. (2005) Evidence for monazite-, barite-, and AgMnO₄ (distorted barite)-type structures in CaSO₄ at high pressure and temperature. *American Mineralogist*, **90**, 22–27.
- Crichton, W.A., Bouvier, P., Winkler, B. and Grzechnik, A. (2009) The structural behaviour of LaF₃ at high pressures. *Dalton Transactions*, **39**, 4302–4311.
- Crichton, W.A., Müller, H., Merlini, M., Roth, T. and Detlefs, C. (2010) Monazite structure from dehydrated CaSeO₄·2H₂O. *Mineralogical Magazine*, **74**, 127–139.
- Crichton, W.A., Merlini, M., Hanfland, M. and Müller, H. (2011) The crystal structure of barite, BaSO₄, at high pressure. *American Mineralogist*, **96**, 364–367.
- Effenberger, H. and Pertlik, F. (1986) 4 monazite type structures – comparison of SrCrO₄, SrSeO₄, PbCrO₄ (crocoite), and PbSeO₄. *Zeitschrift für Kristallographie*, **176**, 75–83.
- Errandonea, D., Kumar, R.S., Achary, S.N. and A.K. Tyagi (2011) *In situ* high-pressure synchrotron X-ray diffraction study of CeVO₄ and TbVO₄ up to 50 GPa. *Physical Review B*, **84**, 224141.
- Forman, R.A., Block, S., Barnett, J.D. and Piermarini, G.J. (1972) Pressure measurement by utilization of ruby sharp-line luminescence. *Science*, **176**, 284–285.
- Fujita, T., Kawada, I. and Kato, K. (1977) Raspite from Broken Hill *Acta Crystallographica Section B: Structural Science*, **33**, 162–164.
- Fukunaga, O. and Yamaoka, S. (1979) Phase transitions in ABO₄-type compounds under high-pressure. *Physics and Chemistry of Minerals*, **5**, 167–177.
- Gracia, L., Beltrán, A., Errandonea, D. and Andrés, J. (2012) CaSO₄ and its pressure-induced phase transitions: a density functional theory study. *Inorganic Chemistry*, **51**, 1751–1759.
- Grzechnik, A., Crichton, W.A., Hanfland, M. and van Smullen, S. (2003) Scheelite CaWO₄ at high pressures. *Journal of Physics: Condensed Matter*, **15**, 7261–7270.
- Grzechnik, A., Crichton, W.A., Bouvier, P., Dmitriev, V., Weber, H.P. and Gesland, J.Y. (2004) Decomposition of LiGdF₄ scheelite at high pressures. *Journal of Physics: Condensed Matter*, **16**, 7779–7786.
- Grzechnik, A., Friese, K., Dmitriev, V., Weber, H.P., Gesland, J.Y. and Crichton, W.A. (2005) Pressure-induced tricritical phase transition from the scheelite to the fergusonite structure in LiLuF₄. *Journal of Physics: Condensed Matter*, **17**, 763–777.
- Hammersley, A.P., Svensson, S.O. and Thompson, A. (1994) Calibration and correction of spatial distortions in 2D detector systems. *Nuclear Instruments and Methods in Physics Research Section A*, **346**, 312–321.
- Hammersley, A.P., Svensson, S.O., Hanfland, M., Fitch, A.N. and Häussermann, D. (1996) Two-dimensional detector software: from real detector to idealized image or two-theta scan. *High Pressure Research*, **14**, 235–248.
- Hazen, R.M. and Finger, L.W. (1982) *Comparative Crystal Chemistry: Temperature, Pressure, Composition and the Variation of Crystal Structure*. John Wiley & Sons, London, 231 pp.
- Hottentot, D. and Loopstra, B.O. (1979) Crystal structures of calcium tellurate, CaTeO₄, and strontium tellurate, SrTeO₄. *Acta Crystallographica Section B: Structural Science*, **35**, 728–729.
- Huang, T., Lee, J.S., Kung, J. and Lin, C.M. (2010) Study of monazite under pressure. *Solid State Communications*, **150**, 37–38.
- Le Bail, A., Duroy, H. and Fourquet, J.L. (1988) Ab initio structure determination of LiSbWO₆ by X-ray powder diffraction. *Materials Research Bulletin*, **23**, 447–452.
- Lee, P.L., Huang, E., and Yu, S.C. (2001) Phase diagram and equations of state of BaSO₄. *High Pressure Research*, **21**, 67–71.
- Lipp, C. and Schleid, T. (2008) Orthorhombisches Sr[SeO₃]. *Zeitschrift für Anorganisches und Allgemeine Chemie*, **634**, 2060–2060.
- Liu, L.-G. (1979) High-pressure phase-transformations in baddelyite and zircon, with geophysical implications. *Earth and Planetary Science Letters*, **44**, 390–396.
- Liu, L.-G. and Bassett, W.A. (1986) *Oxford Monographs on Geology and Geophysics No. 4*. Oxford University Press, New York.
- Long, Y.W., Yang, L.X., You, S.J., Yu, Y., Yu, R.C., Jin, C.Q. and Liu, J. (2006) Crystal structural phase transition in CaCrO₄ under pressure. *Journal of Physics: Condensed Matter*, **18**, 2421–2428.

- Ma, Y.M., Zhou, Q., He, Z., Li, F.F., Yang, K.F., Cui, Q.L. and Zou, G.T. (2007) High-pressure and high-temperature study of the phase transition in anhydrite. *Journal of Physics: Condensed Matter*, **19**, 425221.
- Marques, M., Contreras-Garcia, J., Florez, M. and Recio, J.M. (2009) On the mechanism of the zircon–scheelite pressure induced transformation. *Journal of Physics and Chemistry of Solids*, **69**, 2277–2280.
- Muller, O., White, W.B., and Roy, R. (1969) X-ray diffraction of chromates of nickel, magnesium and cadmium. *Zeitschrift für Kristallographie*, **130**, 112–120.
- Petricek, V., Duskek, M. and Palatinus, L. (2006) *Jana2006. The crystallographic computing system*. Institute of Physics, Praha, Czech Republic.
- Palatinus, L. and Chapuis, G. (2007) *Superflip* – a computer program for the solution of crystal structures using charge flipping in arbitrary space. *Journal of Applied Crystallography*, **40**, 786–790.
- Pistorius, C.W.F.T., and Pistorius, M.C. (1962) Lattice constants and thermal-expansion properties of the chromates and selenates of lead, strontium and barium. *Zeitschrift für Kristallographie*, **117**, 259–271.
- Pistorius, C.W.F.T., Boeyens, J.C.A. and Clark, J.B. (1969) Phase diagram of NaBaF₄ and NaClO₄ to 40 kbar and the crystal-chemical relationship between the structures CaSO₄, AgMnO₄, BaSO₄ and high-NaClO₄. *High Temperature – High Pressure*, **1**, 41–52.
- Reid, A.F. and Ringwood, A.E. (1969) Newly observed high pressure phase transformations in Mn₃O₄, CaAl₂O₄, and ZrSiO₄. *Earth and Planetary Science Letters*, **6**, 205–208.
- Santamaría-Pérez, D., Gracia, L., Garbarino, G., Beltrán, A., Chuliá-Jordán, R., Gomis, O., Errandonea, D., Ferrer-Roca, Ch., Martínez-García, D. and Segura, A. (2011) High-pressure study of the behaviour of the mineral barite by X-ray diffraction. *Physical Review B*, **84**, 054102.
- Snyman, H.C. and Pistorius, C.W.F.T. (1963) Some crystallographic properties of CaSeO₄ and its hydrates. *Zeitschrift für Kristallographie, Kristallgeometrie, Kristallphysik, Kristallchemie*, **119**, 151–154.
- Stephens, D.R. (1964) Hydrostatic compression of 8 rocks. *Journal of Geophysical Research*, **69**, 2967–2978.
- Wildner, M. and Giester, G. (2007) Crystal structures of SrSeO₃ and CaSeO₃ and their respective relationships with molybdomenite- and monazite-type compounds – an example for the stereochemical equivalence of ESeO₃ (E = lone electron pair) with tetrahedral TO₄ groups. *Neues Jahrbuch für Mineralogie*, **184**, 29–37.

